PONTIFICIA UNIVERSIDAD CATÓLICA DEL PERÚ

FACULTAD DE CIENCIAS E INGENIERÍA

ACTIVE NOISE CONTROL FOR MOTORS IN OPERATING RANGE FROM 200 TO 3000 RPM AND NOISE LEVELS AROUND 90 dBA

Tesis para obtener el título profesional de Ingeniero Mecatrónico

AUTOR

Juan Carlos Rajit Lengua Arteaga
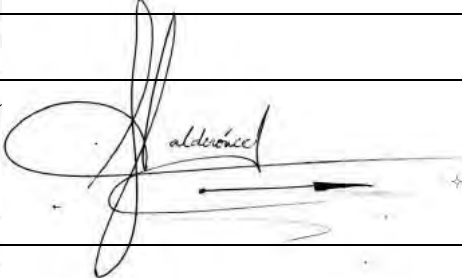
ASESOR:

Jesús Alan Calderón Chavarri

Lima, septiembre, 2018

Informe de Similitud

Yo, Jesús Alan Calderón Chavarri, docente de la Facultad de Ingeniería, Sección Mecatrónica de la Pontificia Universidad Católica del Perú, asesor de la tesis titulada *ACTIVE NOISE CONTROL FOR MOTORS IN OPERATING RANGE FROM 200 TO 3000 RPM AND NOISE LEVELS AROUND 90 dBA*, del autor Juan Carlos Rajit Lengua Arteaga, dejo constancia de lo siguiente:

- El mencionado documento tiene un índice de puntuación de similitud de 18%. Así lo consigna el reporte de similitud emitido por el software *Turnitin* el 07/04/2023.
- He revisado con detalle dicho reporte y la Tesis o Trabajo de Suficiencia Profesional, y no se advierte indicios de plagio.
- Las citas a otros autores y sus respectivas referencias cumplen con las pautas académicas.

Lugar y fecha: Lima Perú, 7 de abril de 2023.

Apellidos y nombres del asesor: Calderón Chavarri, Jesús Alan	Firma
DNI: 43076936	
ORCID: https://orcid.org/0000-0002-6486-5105	

Resumen

La continua exposición al ruido es un mal que podría generar un efecto adverso para la salud. Sin embargo, es considerado como un efecto inherente a los procesos industriales, incluso propio de áreas comerciales en las que es difícil fiscalizar debido al alto tránsito y congestión vehicular. No obstante, en muchos casos se ha tratado de reducir sus efectos utilizando mecanismos pasivos como el uso de materiales absorbentes, los cuales, a pesar de ser efectivos en algunos casos, pueden resultar insuficientes para cancelar ruido a bajas frecuencias. Por otro lado, puede ser impráctico para zonas en las que el espacio es limitado.

En busca de resolver estas desventajas, mecanismos de control activo, en los que es necesario tener fuentes secundarias de sonido, se han desarrollado para la cancelación del ruido mediante interferencia destructiva. Debido a que una segunda fuente de sonido es necesaria, dicha fuente necesitará controlarse mediante un algoritmo que pueda obtener la superposición deseada.

En el presente trabajo, algoritmos de control activo de ruido son analizados, simulados e implementados. Así mismo, se presenta al algoritmo Least-Mean-Square como el más conveniente en control de ruido. Finalmente, motores eléctricos y de combustión interna dentro del rango de 200 a 3000 RPM (revoluciones por minuto), los cuales generan alrededor de 90 dB de ruido, son evaluados.

Abstract

Continuous exposure to noise can generate a detrimental effect in health. However, it is considered as an inherent issue on industrial processes or even on commercial areas where heavy traffic and congestion are difficult to supervise. Hence, it has been tried to be reduced through passive mechanism, such as absorbing materials, which result to be ineffective cancelling low frequencies. Additionally, it could be unpractical when there are space limitations.

In order to overcome these drawbacks, active control approaches have been developed in which a secondary sources array is required to cancel the main source by destructive interference. Due to the fact that a secondary source is expected to be equal in amplitude and opposite in phase, secondary sources need a particular control algorithm to achieve the desired superposition.

In this work active noise control strategies are analysed, simulated and implemented. Furthermore, adaptive algorithm Least-Mean-Square is presented as the most convenient classic control strategies. For this purpose, Diesel and Electric motors under operating range from 200 to 3000 RPM (revolution per minute) are evaluated considering noise levels around 90 dB.

Table of content

List of figures

List of tables

1. INTRODUCTION

1.1 CONTEXT

According to World Health Organization, noise is one of the five main risk factors to health on industrial environments. The evident associated problem is hearing loss which is the most documented. However, there are some others non-auditory effects which are in fact a reaction to noise such as cardiovascular diseases, sleep disturbance, fatigue, or even psychological and psychosocial alterations (Ordaz, et al., 2009).

As inherent effect of industrial processes, noise has been tried to be reduced using passive mechanism such as absorbing materials, double wall glass or earmuffs for workers (Streeter, et al., 2004).

In case of noise in urban areas is slightly more complicated since it depends on traffic, maintenance machinery, among others. Perez Cambra (2015) describe investigations that study influence of vegetation on noise reduction which result to be ineffective at low frequencies and requires space as well as leafy and voluminous plants.

According to records, Active Noise Control idea was born more than 80 years ago when a patent by Paul Lueg explaining the principle was published in 1936. The principle consisted of measuring the sound field in order to send a signal in a secondary source to produce a superposition of two wave which results in destructive interference (Elliot & Nelson, 1993). However, the lack of technology to apply this principle delayed its study.

Afterwards, the development of digital signal processing, as well as improved DSP hardware and transducers, meant the progress of ANC (Active Noise Cancellation) and development of new algorithms (Kuo & Morgan, 1999). Nowadays, as technology allowed it, ANC has taken advantage of its excellent performance at low frequencies against passive mechanism. Sometimes, both mechanisms, passive and active, are used simultaneously to improve attenuation (Streeter, et al., 2004).

Then, it is convenient to implement some strategies against noise, especially in areas which are in presence of engines, cars, fans, compressors, electrical motors, among others.

In Peru, according to supreme decree N° 085-2003-PCM, there are some permissible limits of noise which is classified in 4 zones and 2 schedules (Presidencia del Consejo de Ministros, 2003), as it is shown in Table 1.1.

Table 1.1: Limits of noise in Peru (Organismo de evaluación y fiscalización ambiental, 2016)

APPLICATION ZONE	Values in dB (A)	
	Day Schedule (7:01 – 22:00)	Night Schedule (22:01 – 7:00)
Special zone	50 dB	40 dB
Residential zone	60 dB	50 dB
Commercial zone	70 dB	60 dB
Industrial zone	80 dB	70 dB

However, according to *Organismo de Evaluación y Fiscalización Ambiental* (Abbreviated to OEFA in Spanish), which is in charge of promoting compliance of environment obligations, this rule is far of complying. The evidence is shown in Table 1.2 which describes places in Lima city and Callao that are off-limits.

Table 1.2: Places with high level of noise in Lima and Callao (Organismo de evaluación y fiscalización ambiental, 2016)

Pos.	Distrito	Descripción	Nivel de ruido (dBA)
1	El Agustino	Av. Jose Carlos Mariátegui	84.9
2	Santiago de Surco	Av. Javier Prado	84.5
3	Ate	Carretera Central	84.3
4	San Martin de Porres	Municipalidad de San Martin de Porres	83
5	Lurigancho	Av. Las Torres	82.7
6	El Agustino	Av. Riva Agüero	82.3
7	Carabayllo	Av. Merino Reyna	82.2
8	San Juan de Miraflores	Av. Los Héroes	81.9
9	Santiago de Surco	Av. Santiago de Surco	81.8

10	Breña	Plaza Bolognesi	81.6

There are approximately 215 places, besides the mentioned ones, where the noise is greater than the set limit according to *OEFA*.

Furthermore, council of Lima monitored noise in Lima District and elaborated a map of noise, shown in Figure 1.1. Red zones are between 75 - 80 dB and orange zones between 70 and 75 dB which is evidence that rules are not followed.

Figure 1.1: Map of noise – Lima District (Municipalidad de Lima, 2019)

1.2 GENERAL OBJECTIVE

Design and implement an Active Noise Control system based on Least-Mean-Square algorithm destined to Electrical and Diesel motors under operating range from 200 to 3000 RPM.

1.3 SPECIFIC OBJECTIVES

- Evaluate the performance of a system that captures noise and sends antinoise signal through a speaker.
- Record noise from Electrical and Diesel motors in order to simulate system identification using Least-Mean-Square.
- Test the Lest-Mean-Square algorithm at different speeds.
- Verify noise reduction in specified range.

2. STATE OF THE ART

This chapter contents basics concepts of sound and how people are affected by noise. Additionally, a presentation of active noise control and the relevance of adaptive filter algorithm application as well as a briefly description on the recent advances in active noise control.

2.1 THEORETICAL FRAMEWORK

2.1.1 SOUND AND PERCEPTION

Sound is a physical effect produced by a wave propagation through an elastic medium so that it has two requirements, one is the compressibility that makes the media, such as air or water, tend to return its original state; and the inertia of the mass which causes the motion to overshoot.

Figure 2.1 illustrates the sound propagation in 3-dimensional space from a source *Q(r,t)* which is transmitted at *C* speed. It should be noticed that source generates a pressure field *P(r,t)* given by Equation 2.1 (Zangi, 1994).
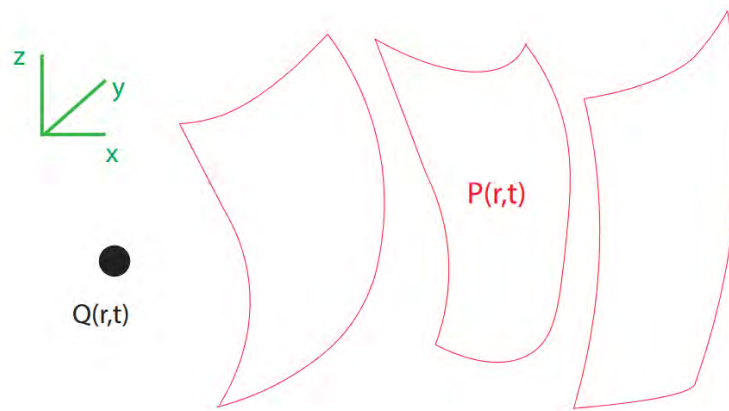
Figure 2.1: Mechanical wave propagation

$$\frac{1}{C^2}\frac{\partial^2}{dt^2}P(r,t) - \nabla^2 P(r,t) = Q(r,t) \; . \tag{2.1}$$

This physical effect has two main attributes which are loudness, identified by sound pressure; and timbre, distinguished by wave frequencies. In the case of audible frequencies, the hearing range is about between 20 Hz to 20000 Hz (16 to 16000 Hz for some authors). However, it cannot be defined precisely as it depends on some individually factors such as age, wide noise exposure or misuse of sound devices (Möser, 2009). On the other hand, it is important to recognise a minimum audible sound which is accepted as 2.10^{-5} Pa. Having said that, a limit could be defined below 200 Pa (pain threshold).

As it is explained, the sound pressure perception range is wide. Then it is more manageable to use the logarithmic measure shown in Equation 2.2, which is internationally accepted.

$$L = 20 \log\left(\frac{p}{p_0}\right).$$

(2.2)

Where p is sound pressure and $P_0 = 20.10^{-6}$ Pa is a reference of the hearing threshold at a frequency of 1 kHz.

The frequency of 1 kHz is used as reference because the sensitivity of human ear depends on the tonal pitch. The array of curves presented in Figure 2.2 is called hearing levels and shows that when a 1 kHz tone is compared to a second tone of different frequency, it is necessary to adjust the level of the second one in order to perceive it with the same loudness (subjective loudness).

Not only that, *perception loudness* is also dependent on the bandwidth of the sound. For this reason, it is commonly seen in practical applications to measure sound using the A- filter in dB (A). The A-filter response is shown in Figure 2.3; filters B-, C- and D- which are used for special applications are also presented.
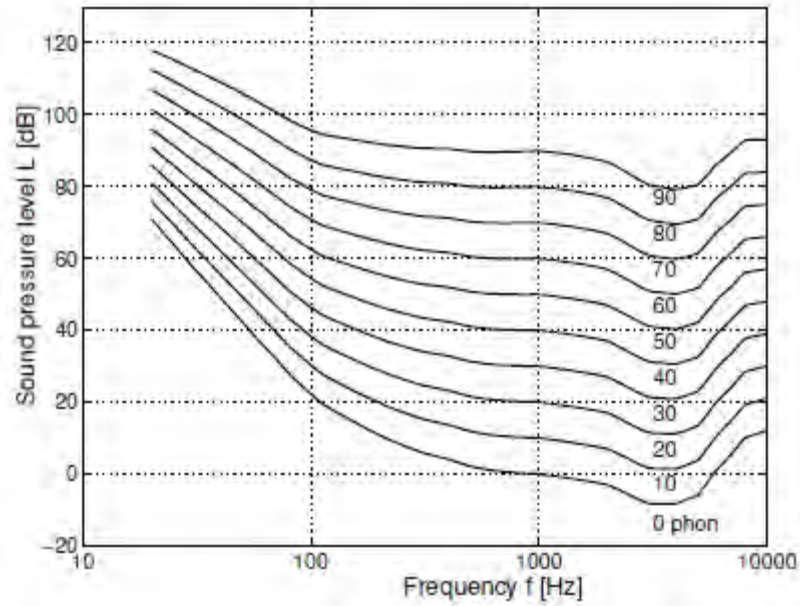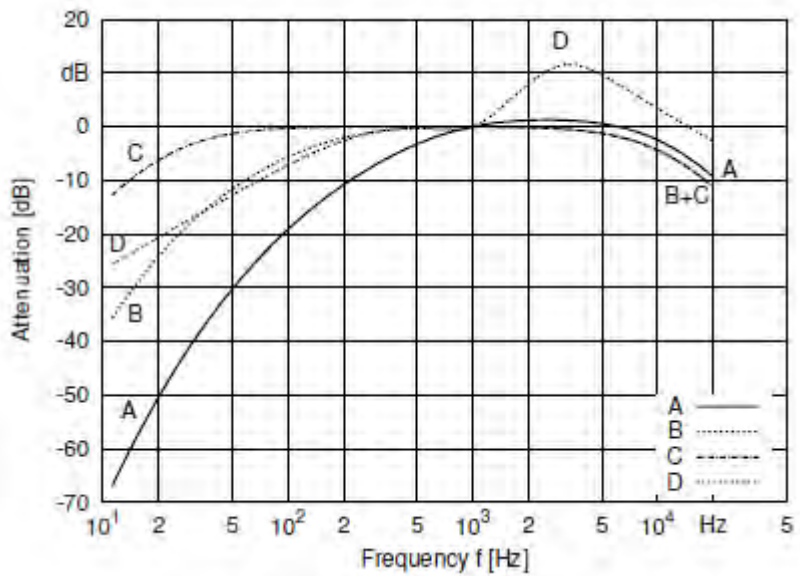
Figure 2.2: Hearing levels (Möser, 2009)

Figure 2.3: Frequency response of A-, B-, C-, and D-weighting filters (Möser, 2009)

2.1.2 NOISE EFFECTS

Although continuous noise exposure causes many adverse effects, it is a known problem among people working in industry. Noise frequency from machinery is usually below 2 kHz (Keelara Veerappa & Venugopalachar, 2011).

Keerlera & Venufopalachar (2011) studied the possible influence of noise frequency on industrial environment. Table 2.1 shows some of their recompilation.

Table 2.1: Reviewed studies on noise effects (Keelara Veerappa & Venugopalachar, 2011)

Noise Level	Noise characteristics	Frequency Analysis	Auditory Effects	Non-auditory effects
87-90 dB (A)	Quasi-steady state, impulsive	1-3 kHz	Significant loss of 25 dB at the analysed frequency	
87-125 dB (A)	Steady-state, impact noise	4 kHz	Affects hearing threshold at frequency	
75-104 dB (A)	Broad band noise	-	-	Systolic blood pressure > 160 mmHg
> 85 dB (A)		-	-	Diastolic blood pressure > 95 mmHg
75-85 dB (A) 95-110 dB (A)	Turbine noise	4-6 kHz	Noise-Induced Hearing Loss (56 % investigated)	
>80 dB (A)	-	-	-	Diastolic and systolic blood pressure changes
> 90 dB (A)	-	-	High frequency noise induced threshold shifts (25 % permanent)	
71-98 dB (A)	-	-	-	Systolic blood pressure significantly high
> 85 dB (A)		4 kHz	Significant evidence of noise induced hearing loss	-
80-96 dB (A) 78-98 dB (A) 88-95 dB (A)		-	Hearing loss	Sleep disturbance
95 dB (A)	Continuous and steady recorded		Temporary threshold shift is enhanced by stress and workload	

81-108 dB (A)	Continuous, impulsive, intermittent, hammering, welding	0.0315 - 2 kHz Octave band centre	Hearing problems 88-707 Hz	Cardiovascular problems at 354 - 707 Hz

2.1.3 ACTIVE NOISE CONTROL

Active noise control is a method which consists of creating an anti-noise source in order to cancel a primary noise. It is based on superposition of the primary noise and the anti-noise which should have same amplitude and opposite phase. For this purpose, three main components are required according to Bies & Hansen: "The control signal, given by the controller; the sensor signal, which is the input for the controller; and the actuator, which is in charge of converting signals of the controller into sound" (Bies & Hansen, 2003). Figure 2.4 shows a common feedback noise control system which essentially consists of a low pass filter and an amplifier. The error sensor output is processed in order to generate the secondary signal.
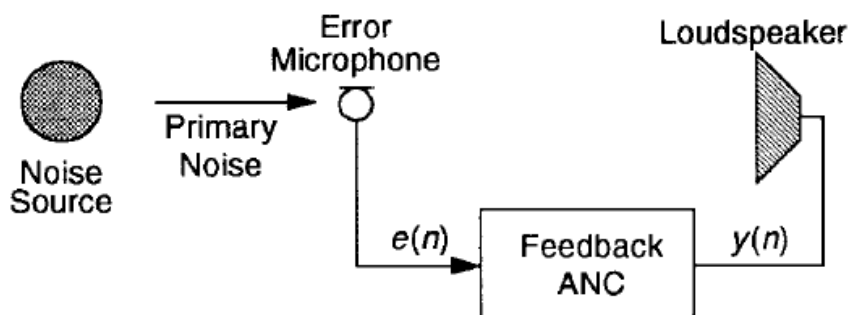
Figure 2.4: Feedback ANC System (Kuo & Morgan, 1999)

Noise has time varying characteristics such as the amplitude, frequency and sound velocity which are nonstationary. To deal with these variations, the system should be adaptive to track it (Kuo & Morgan, 1999).

2.1.3.1 ADAPTIVE FILTERING APPLICATION

Adaptive filters, known as self-designing filters, are commonly used in applications where the signals that compose the system are not well defined, not available or time varying due to the fact that they perform on-line updating of its coefficients. Figure 2.5 shows a general block-diagram of an adaptive filter.

Main adaptive filtering applications includes system identification, channel equalization, signal enhancement and prediction (Diniz, 2008). For noise control purpose, it is important to analyse system identification, which is shown in the block diagram in Figure 2.6, as the characteristics of the noise source and environment are non-stationary, that is to say, phase, frequency, amplitude and sound velocity are time varying.
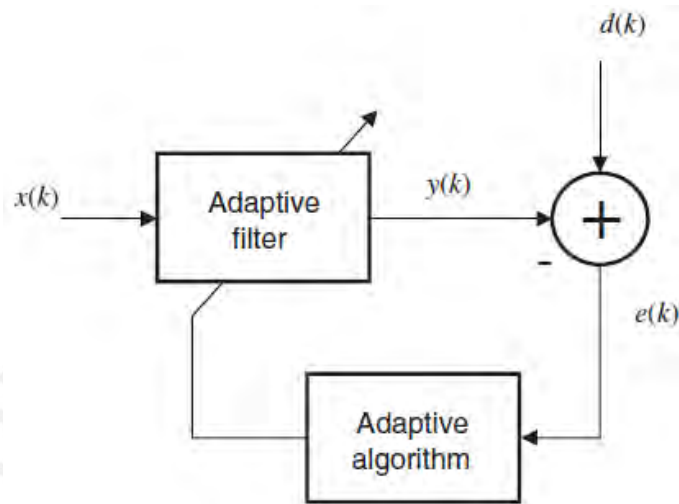

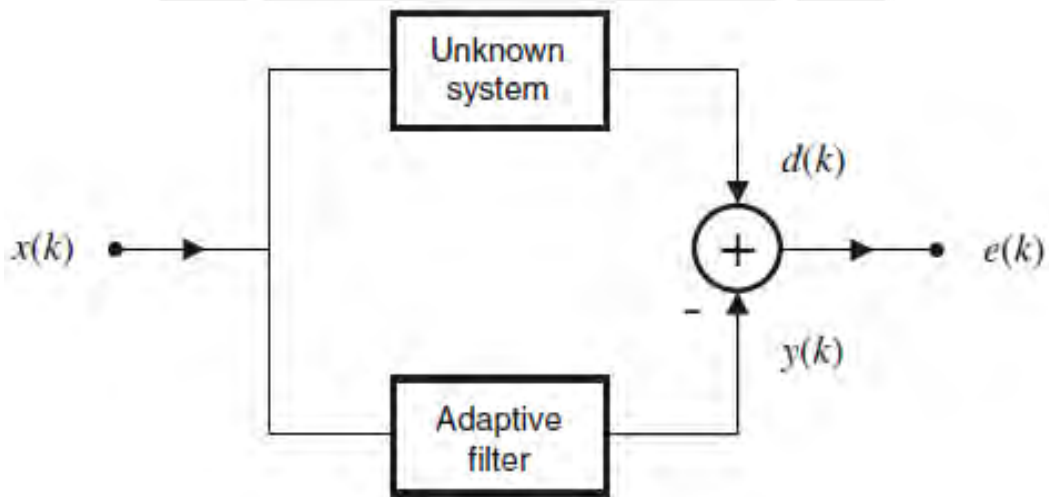Figure 2.5: General adaptive-filter (Diniz, 2008)

Figure 2.6: System identification block diagram (Diniz, 2008)

While classic control approach such as PID(Proportional-Intregral-Derivative) tries to reduce the error, which is the subtraction of reference signal and feedback signal, the idea of using an adaptive filter is to estimate the noise to use it as a reference. Therefore, an adaptive control is the suitable choice.

9

2.1.4 LEAST MEAN SQUARED ALGORITHM

The Least Mean Square (LMS) is an algorithm which is wide used in adaptive filter analysis due to its computational simplicity and robustness. An LMS filter is depicted in Figure 2.7. Basically, the LMS sequential procedure is used to adapt the tap weights. Then, the filter output is given by the following Equation 2.3, which is the transversal structure (Farhang-Boroujeny, 2013) .
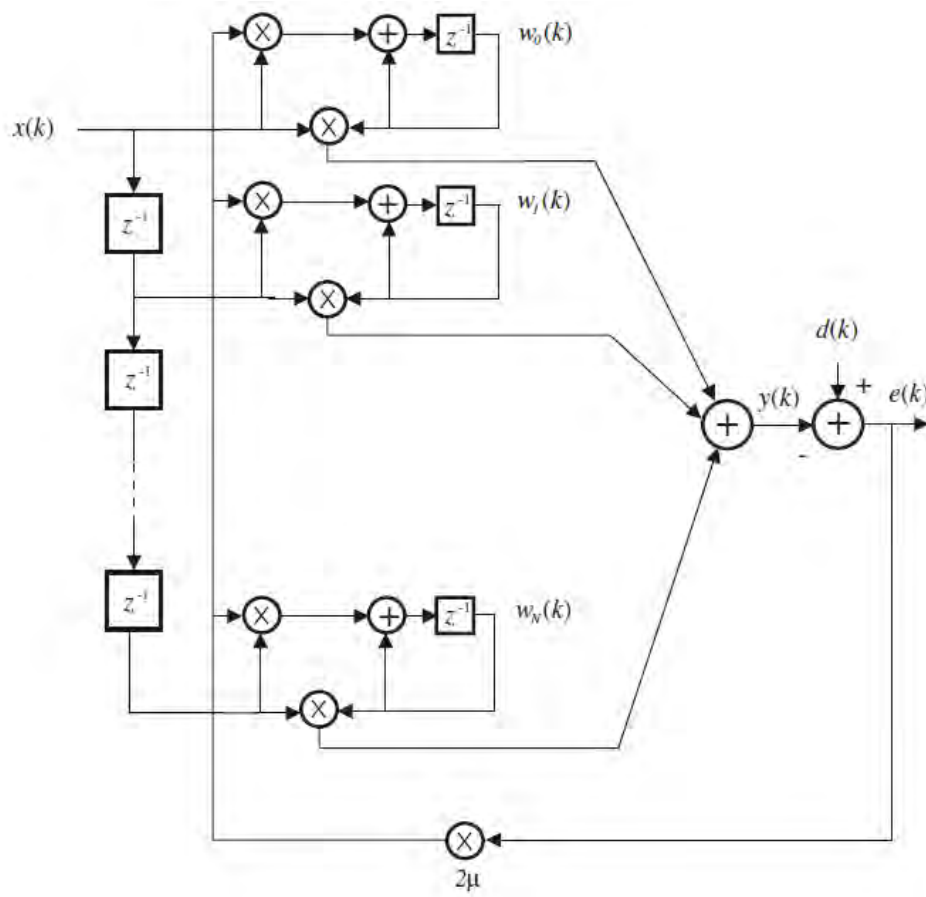

Figure 2.7: LMS adaptive filter (Diniz, 2008)

$$y(n) = \sum_{i=0}^{N-1} w_i(n)x(n-i).$$

(2.3)

Where N is the up limit of the summatory, i is the auxiliary variable, moreover the tap-weights w_i depends on time "n", which is evident that in general the tap-weights are time varying, and they have to be adjusted in an iterative process in order to track every signal variation. The error estimation is calculated by Equation 2.4.

$$e(n) = d(n) - y(n).$$

(2.4)

As mentioned, an update of the coefficients is needed. So that, it is necessary a third equation that depends on weights $w_i(n)$ to complete the LMS algorithm. For this objective, the cost function J (which is represented by Figure 2.8) should be analysed.
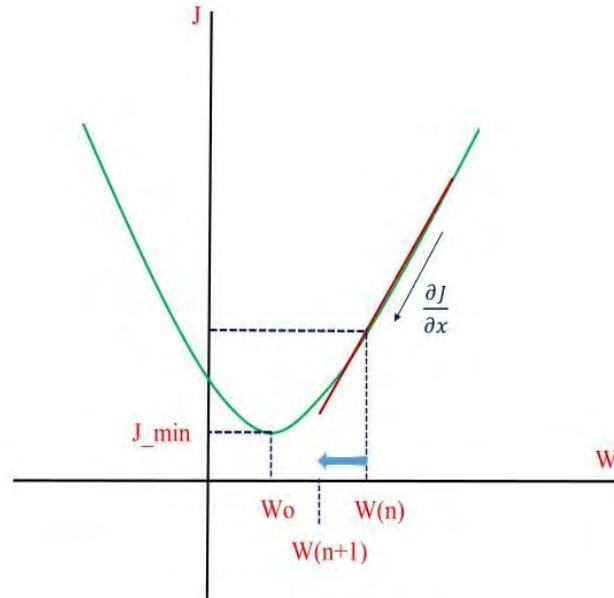

Figure 2.8: Cost Function representation (Calderón, et al., 2019)

As the cost function is defined by mean-squared error e^2, value of $w(n+1)$ would be determined by the following equation.

$$w(n + 1) = w(n) + \mu e^2. \tag{2.5}$$

Replacing the cost function by its derivative respect to weights in order to find the optimal weight matrix (Kuo & Morgan, 1999), (Calderón, et al., 2019):

$$w(n + 1) = w(n) + \mu \frac{\delta(e^2)}{\delta w}. \tag{2.6}$$

$$w(n + 1) = w(n) + \mu \frac{\delta(e^2)}{\delta w} \frac{\delta e}{\delta e}. \tag{2.7}$$

$$w(n + 1) = w(n) + \mu \frac{\delta(e)^2}{\delta e} \frac{\delta(d - w)}{\delta w}. \tag{2.8}$$

11

As desired value *d* does not depend on matrix *w:*

$$w(n+1) = w_n - \mu \frac{\delta(e^2)}{\delta e} \frac{\delta(w)}{\delta w}.$$

(2.9)

And finally, Equation2.10 is obtained:

$$w(n+1) = w(n) + 2\mu e(n)x(n).$$

(2.10)

It is important to mention that sign has been changed in order to follow references of some authors (Farhang-Boroujeny, 2013). Error *e* could take negative or positive values.

To sum up, it requires the three steps mentioned as Equation 2.3, which is the filter; Equation 2.4, which is the error estimation; and Equation 2.10, which is referred to adaptation of coefficients. This last equation also probes the LMS recursion.

2.1.4.1 NORMALISED LEAST MEAN SQUARE

LMS algorithm has a main disadvantage which is the slow rate of convergence. As it could be ineffective to estimate the input correlation matrix, it would be possible to have a variable convergence factor which is what the Normalised Least Mean Square (NLMS) Equation 2.11 shows the evaluation of the variable convergence factor.

$$\mu(n) = \frac{\mu_n}{\gamma + x^T(n)\,x(n)}.$$

(2.11)

Where μ_n is the step which is introduced to control the misadjustment due to the fact that all derivations are based on instantaneous values of the squared errors and not MSE (Diniz, 2008) and should satisfy $0 < \mu_n < 2$; γ is a positive number that solve a problem that occurs when x(n) is small to avoid large step sizes.

The NLMS typically converges faster than the LMS as the aim of using a variable convergence factor is to minimise the output error. The adaptation of the coefficients is calculated using Equation 2.12

$$w(n+1) = w(n) + \frac{\mu_n}{\gamma + x^T(n)\,x(n)} e(n)x(n).$$

(2.12)

2.1.4.2   FILTERED-X LEAST MEAN SQUARE

Filtered-x Least Mean Square (FxLMS) algorithm, which block diagram is shown in Figure 2.9, is a variation of LMS. By itself LMS requires a secondary path transfer function S(z), which includes D/A converter, reconstruction filter, power amplifier and loudspeaker, placed following the digital filter W(z) for compensation (Kuo & Morgan, 2000). This aggregate could cause instability because the error signal is not aligned in time with reference signal. For this reason, it is suggested to place an identical filter S^(z) between the reference signal and the adaptation algorithm what is actually the FxLMS algorithm.
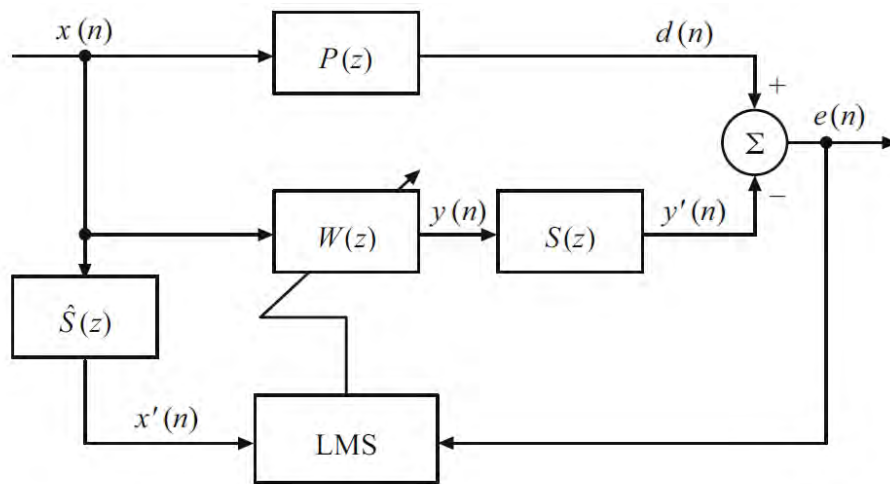
Figure 2.9: Filtered-X LMS block diagram for ANC system (Kuo & Morgan, 2000)

According to find weight matrix *w,* from a XLMS filter, it was analysed the error by Least-mean-square, which are described by Equation 2.13 and Equation 2.14.

$$e(n) = d(n) - s(n) * [w^T(n) \, x(n)]. \tag{2.13}$$

$$w(n + 1) = vw(n) - \mu x'(n)e(n). \tag{2.14}$$

Where $v = 1 - \mu\gamma$ is the leakage factor that should satisfy $0 < v < 1$

2.2 PRELIMINARY STUDIES

2.2.1 ADAPTIVE CONTROL EXPERIMENTATION

Chen, Chang, & Kuo (2017) worked with a system composed by a 6 inches diameter PVC duct shown in Figure 2.10.

Figure 2.10: Duct system (Chen, et al., 2017)

For experimentation, authors have applied a feedforward ANC system with a FXLMS algorithm. As it is shown, an extra microphone is used to measure the noise signal which means this is a feedforward system. They pointed that a feedforward system is more convenient for a non-periodical noise signal than feedback system.

Table 2.2 shows the result of the algorithm with four different noise sources. A 350 Hz single-tonal noise; a multi-tonal noise with 350 Hz, 450 Hz, 550 Hz and 650 Hz; a sweep sine signal conformed by 15 tonal within 200 to 700 Hz; and white noise.

Table 2.2: Noise reduction in dB (Chen, et al., 2017)

Noise type	ANC OFF	ANC ON	Noise Reduction
Single-tonal noise	86	60	26
Multi-tonal noise	80	60	20
Sweep sine signal	86	64	22
White noise	88	66	22

Luo, Sun, Huang & Bai (2017) tested a recursive feedback ANC system shown in Figure 2.11 using filtered-s least mean square (RFSLMS) for chaotic noise. Moreover, they compared FXLMS algorithm to probe it can be less effective under nonlinear and wideband noise like chaotic one.

Additionally, the total number of multiplications required is $(N1 + N2)(2P+1)(M+3)$ and $(N1 + N2)(2P+2)(M+1)$ for addition, where $N1$ is the length of feedforward section, $N2$ the length of the feedback and P is the order of trigonometric expansion. It seems to be similar to the complexity reached by FSLMS. However, the difference

consists in using less memory (N1+N2) as it is a recursive feedback system. Some of the results are shown in the comparative graph in Figure 2.12.
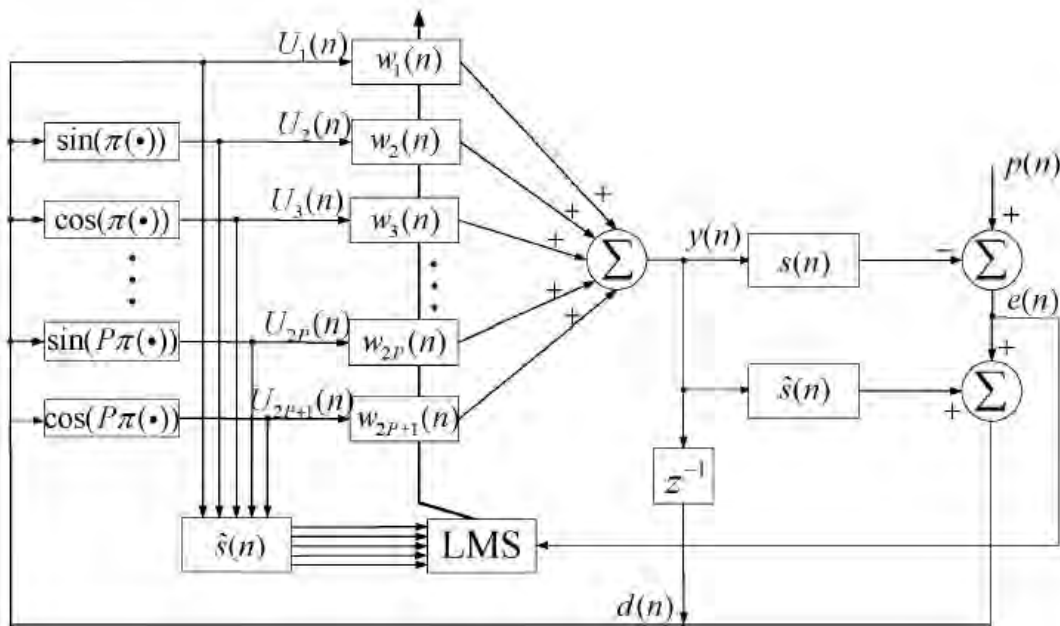

Figure 2.11: Feedback ANC system using RFSLMS (Luo, et al., 2017)
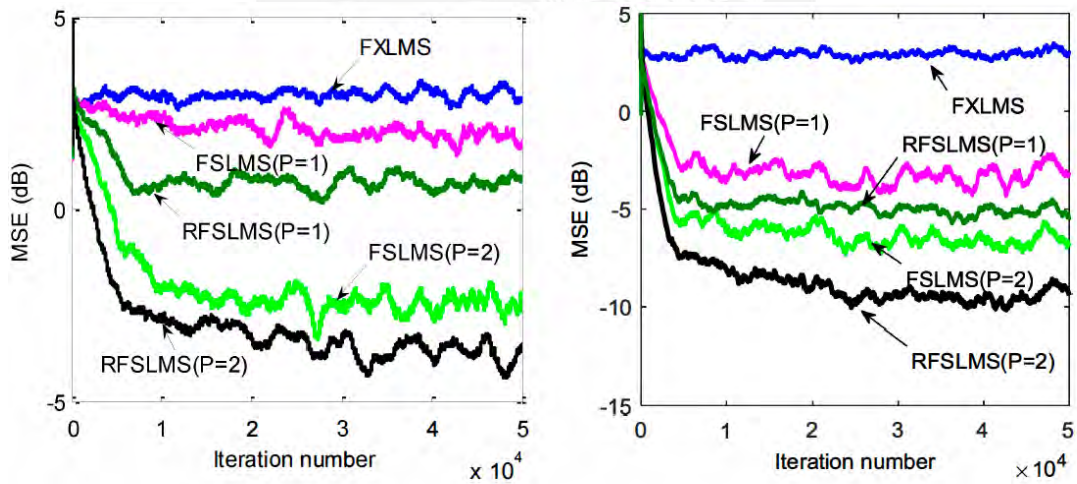

Figure 2.12: Results of different algorithms (Luo, et al., 2017)

Jin Fan (2010) tested the FXLMS algorithm in a pump house located in a mine tunnel in which the noise reaches up to 95 dBA. The major frequencies identified by FFT

(Fast Fourier Transformation) were 23, 51, 102, 207, 433 and 621 Hz. Results using normalized frequency are depicted in Figure 2.13.
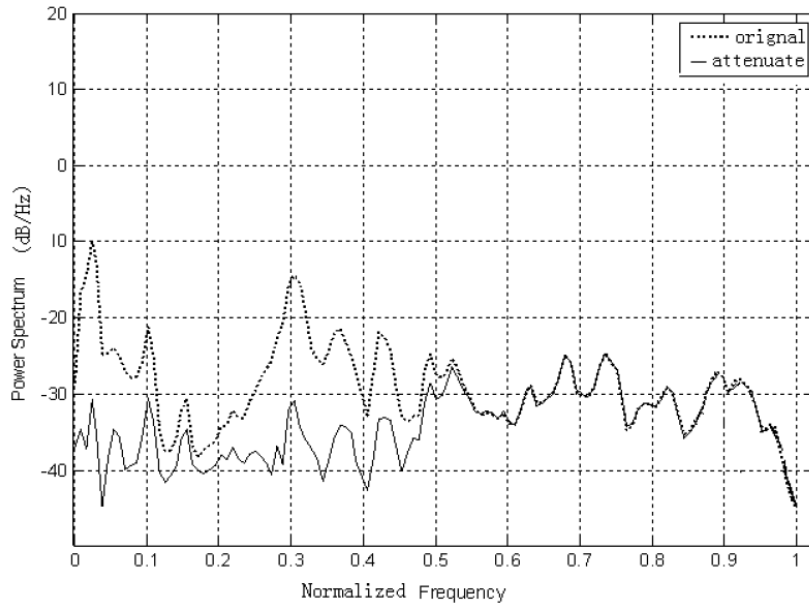

Figure 2.13: Comparison between original signal vs attenuated signal (Luo, et al., 2017)

Mohapatra & Kar (Mohapatra & Kar, 2015) proposed a feedback FXLMS algorithm which is illustrated in Figure 2.14. Both conventional FXLMS and feedback proposed FXLMS were tested offline and online with the exactly same noise and the results are shown in Figure 2.15 and Figure 2.16.
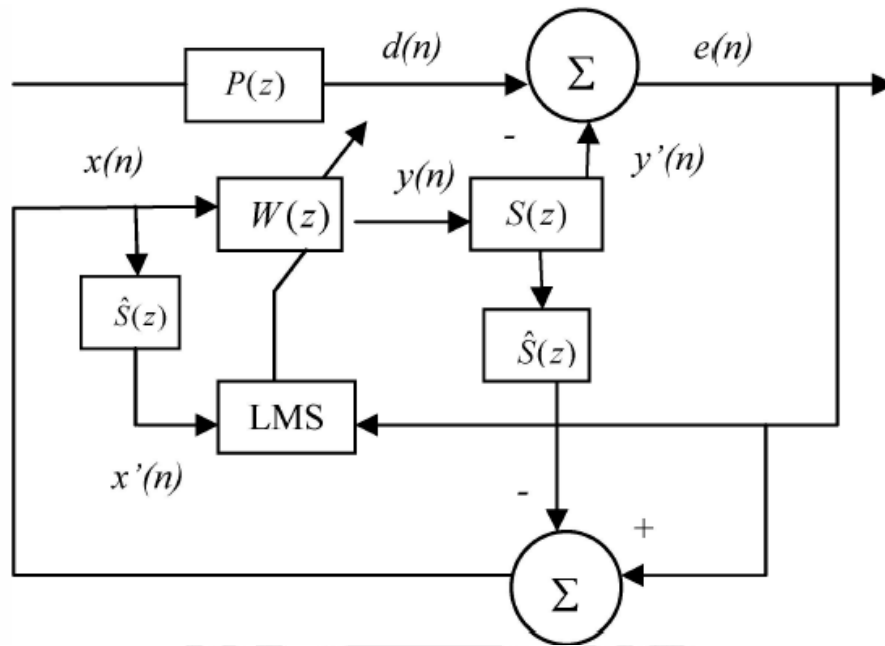
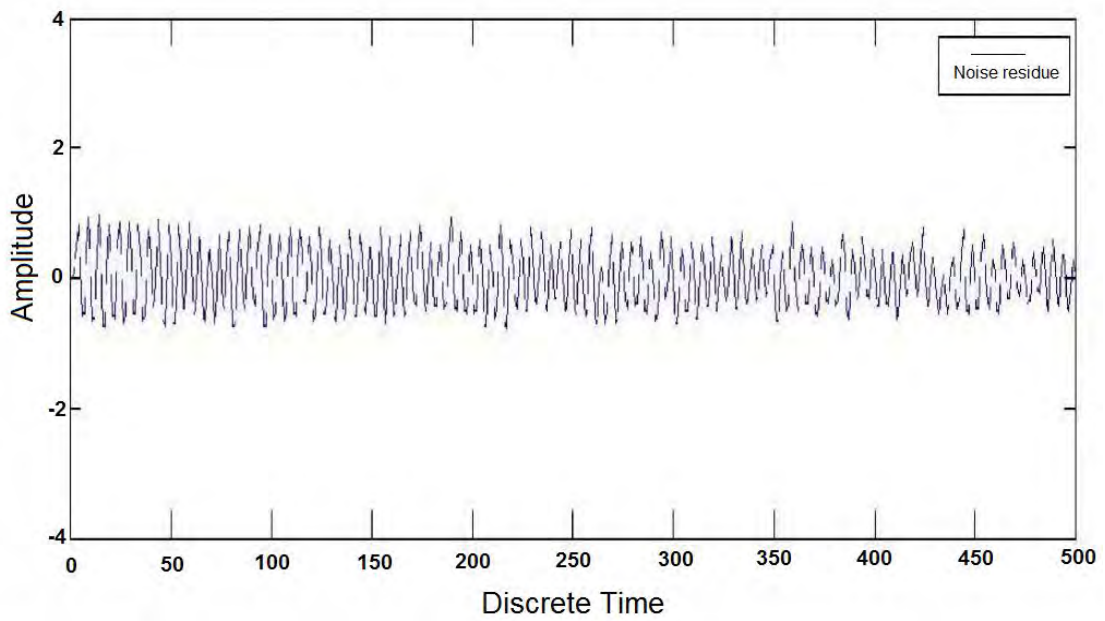Figure 2.14: Feedback FXLMS ANC Structure (Mohapatra & Kar, 2015)

Figure 2.15: Noise residue reached using feedback FXLMS (Mohapatra & Kar, 2015)
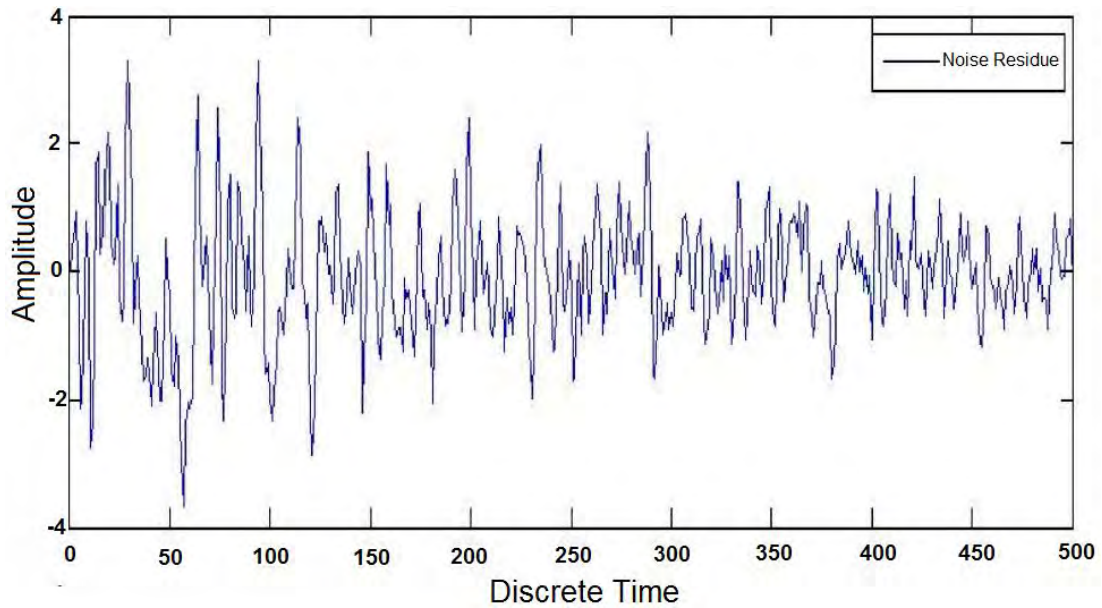
Figure 2.16: Noise residue reached using conventional FXLMS (Mohapatra & Kar, 2015)

It is evident that the algorithm proposed by the authors improve the estimation and adaptation in this specific experiment.

Streeter, Ray & Collier (2004) performed experiments using feedback, feedforward and a hybrid feedforward-feedback algorithm shown in Figure 2.17. For its evaluation, different noise sources were selected: a sum of tones signal comprised of 1/3-octave pure between 50 and 800 Hz; F-16 cockpit noise limited between 50 and 800 Hz and Huey helicopter noise likewise band-limited between 50 and 800 Hz. In addition to that, experiments were made in earmuffs, so the algorithm were tested using both passive and active mechanism. First, passive mechanisms were tested and then a combination of active and passive were tested in order to obtain, by subtraction, attenuation accomplished by active algorithm.
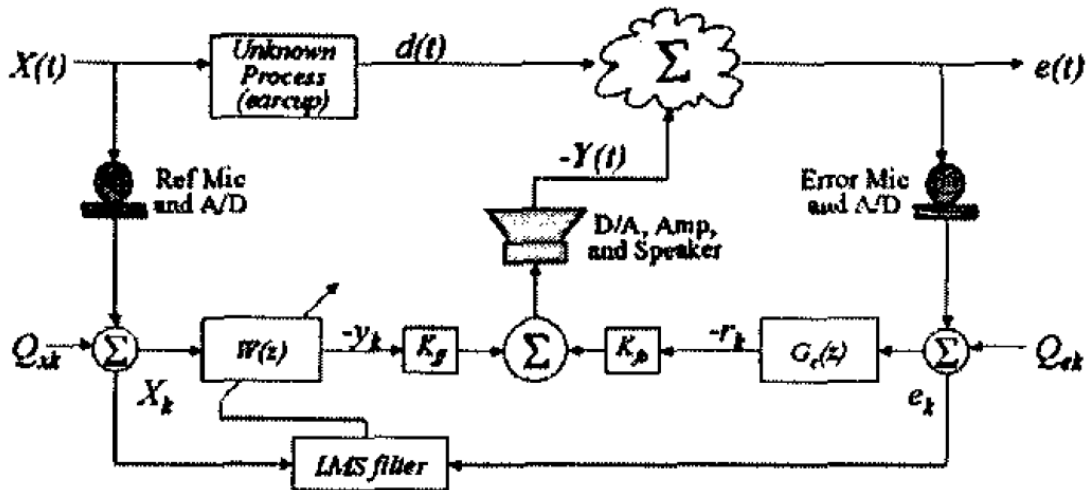
Figure 2.17: Combined feedforward-feedback topology (Streeter, et al., 2004)

Results depicted in Table 2.3 show that feedback has low attenuation (5-10 dB), but authors pointed up that has a high bandwidth attenuation capabilities. On the other hand, feedforward accomplishes remarkably well from 80 to 400 Hz. Furthermore, combined system provides a better performance and works for a frequency range from 40 to 1250 Hz. When the source level is around 110 dB, the noise level inside the earcup is reduced by 36 to 51 dB within the mentioned band.

Table 2.3: Active noise results (Streeter, et al., 2004)

Noise Source	Noise level (dB)	Total Active Attenuation (dB)		
		Feedback	Feedforward	Hybrid
Sum-of-tones 50-800 Hz	110.3	7.8	16.6	27.2
F-16 Cockpit 50 -800 Hz	110.3	7.9	9.8	17.3
Huey Cockpit 50-800 Hz	105.3	8.2	10.5	18.4

3. SYSTEM IDENTIFICATION

In this chapter, experimental analysis has been made using different motors in order to achieve a system identification. Simulations are also presented.

In the following tests, the microphone receives the noise signal from the motor and the controller send the inverse signal though the speakers. Noise signal is obtained by switching off the speakers, then the error is measured by switching on the speakers so that the noise signal and error signal tend to have an offset as it is seen in the results figures which are a comparison between the noise and error after sending the anti-noise signal.

3.1 EXPERIMENTAL ANALYSIS ON AC MOTOR USING REAL-TIME SYSTEM

Hardware configuration is depicted in Figure 3.1: two speakers, a single microphone and AC motor are used for this analysis. Control is made using an FPGA programmed in LabVIEW and results are shown for different speeds.

Figure 3.1: Hardware settings for system identification on AC motor

A comparison between noise and error are shown in Figure 3.2, Figure 3.3, Figure 3.4 and Figure 3.5. "Noise" is produced by the AC motor while "Error sending antinoise"

is the result of superposition of noise and sound produced by the speakers. As it seems, an offset is presented and the reduction is almost imperceptible. However, the data obtained from the noise is relevant to make a system identification.
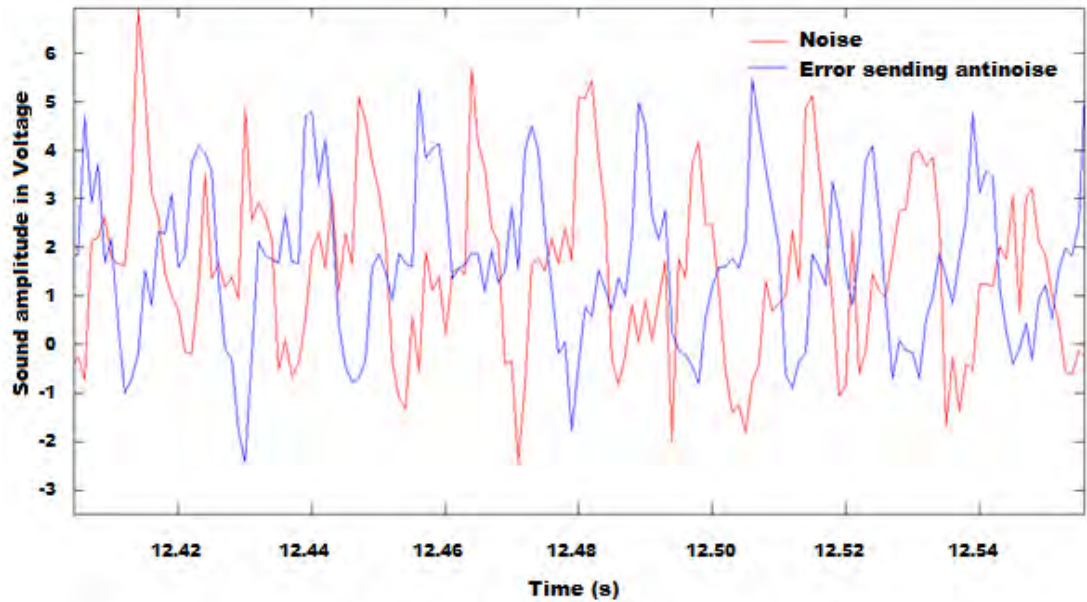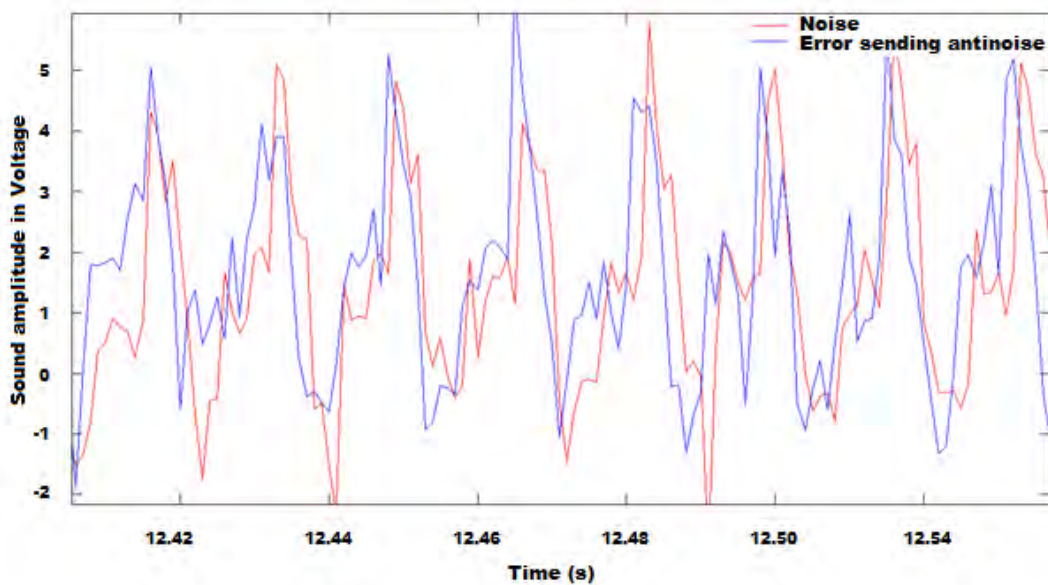

Figure 3.2: AC motor Test at 280 RPM

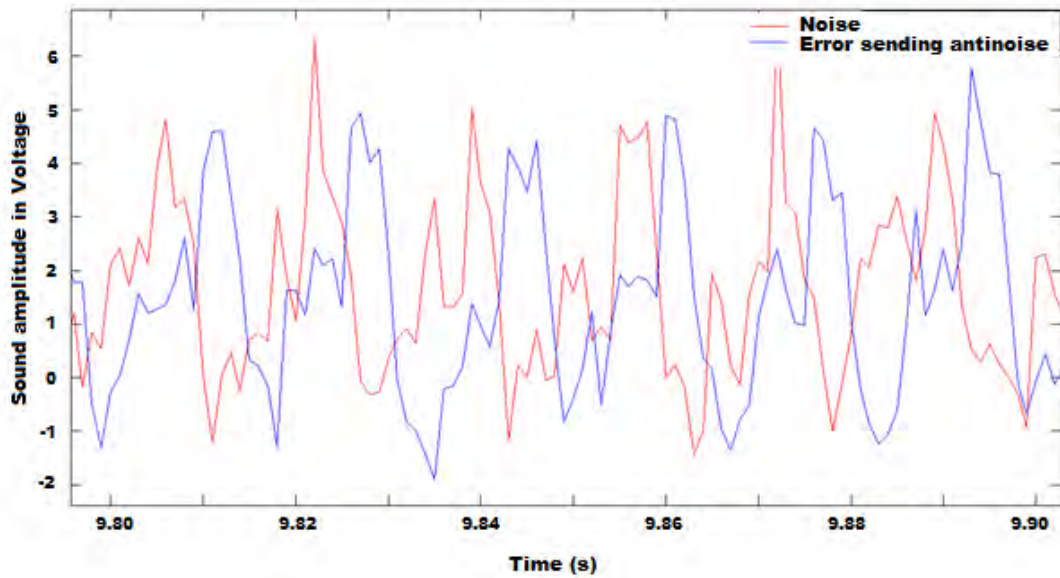Figure 3.3: AC Motor test at 550 RPM
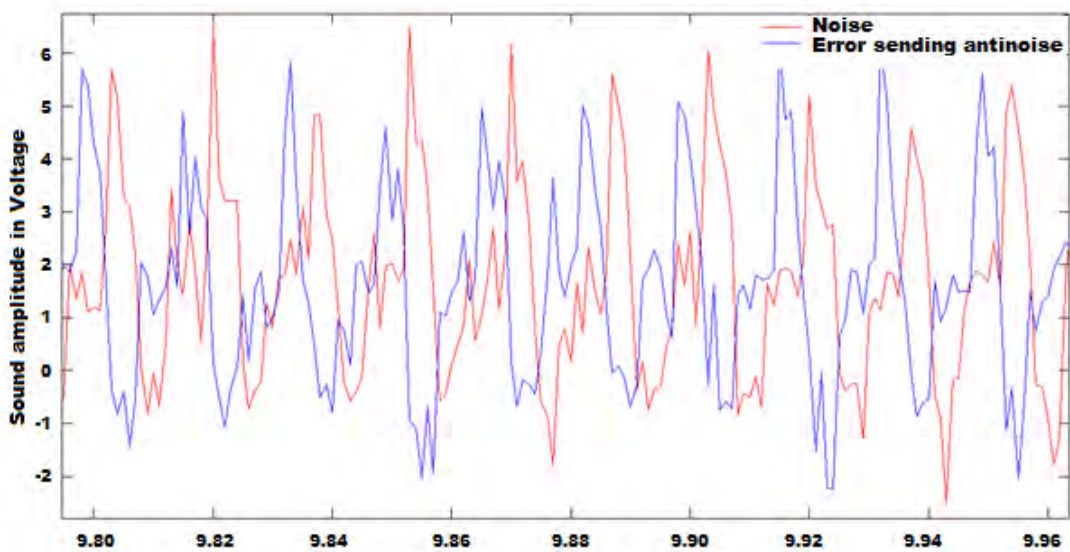
Figure 3.4: AC Motor Test at 820 RPM

Figure 3.5: AC Motor Test at 1093 RPM

On the other hand, Figure 3.6 displays noise levels obtained after sending the anti-noise. Nevertheless, results with no algorithm shows a reduction around 2 dBA which is a poor solution. It means that a control algorithm is needed in order to get a better error.
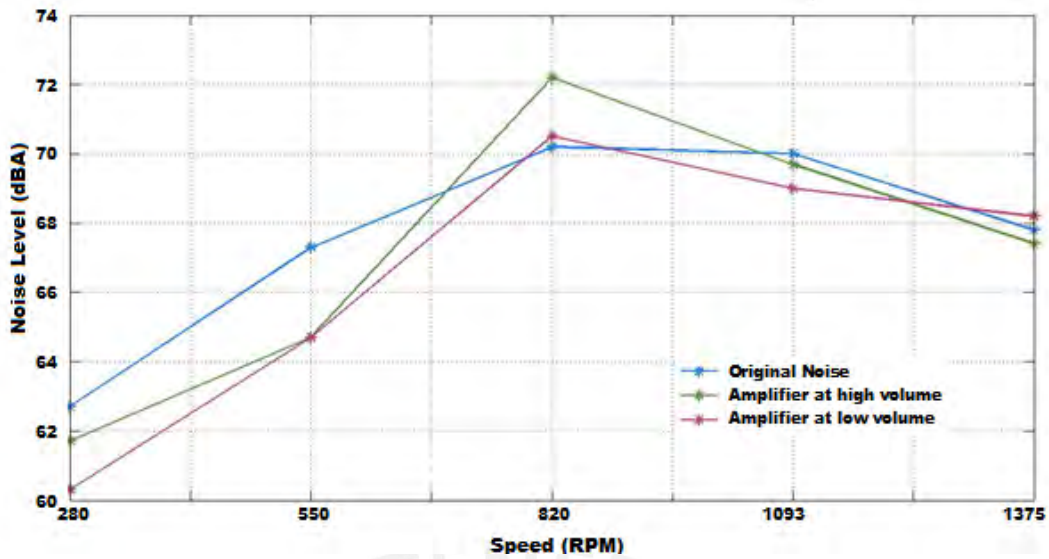
Figure 3.6: Noise reduction for different speeds

3.1.1 SYSTEM IDENTIFICATION USING LMS

Noise data stored from experimental analysis is used to get the weights that represents the Plant of the system via LMS algorithm on a MATLAB script. The step used for this purpose is μ=0,001.

Following results are obtained by simulations. Identified error, shown in Figure 3.7 Figure 3.8, Figure 3.9 and Figure 3.10 are presented for each speed of the motor. In average, the attenuation is about 14 dB in the first case (Figure 3.7).
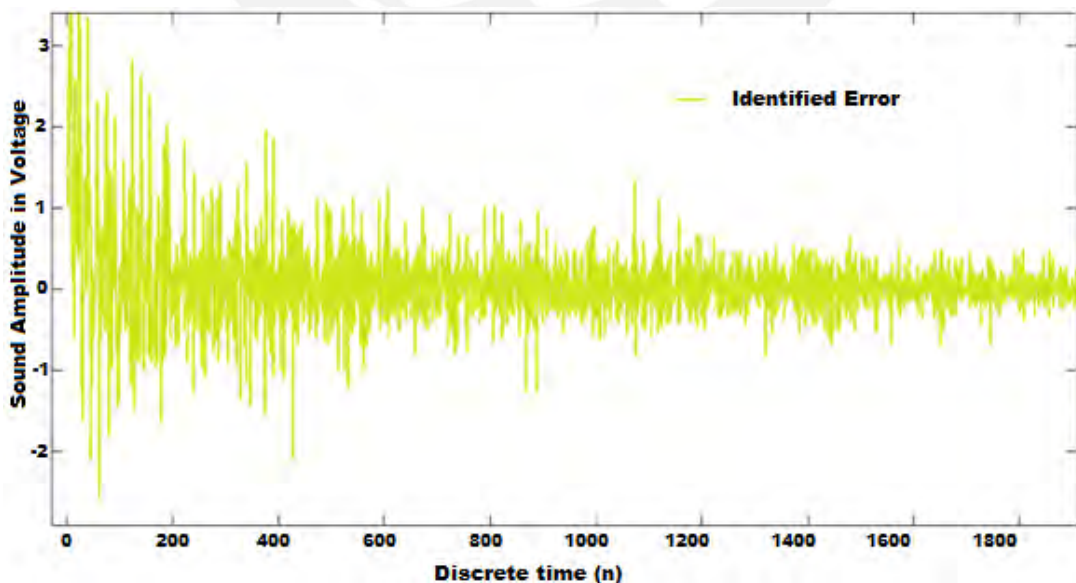

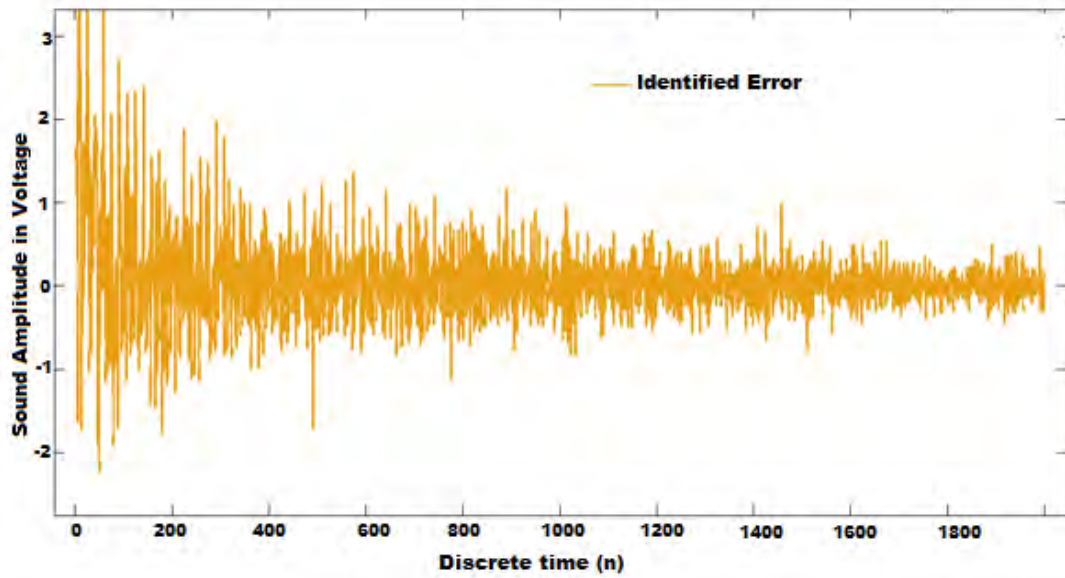Figure 3.7: Identified Error for an AC motor operating at 280 RPM

23

Figure 3.8: Identified Error for an AC motor operating at 550 RPM

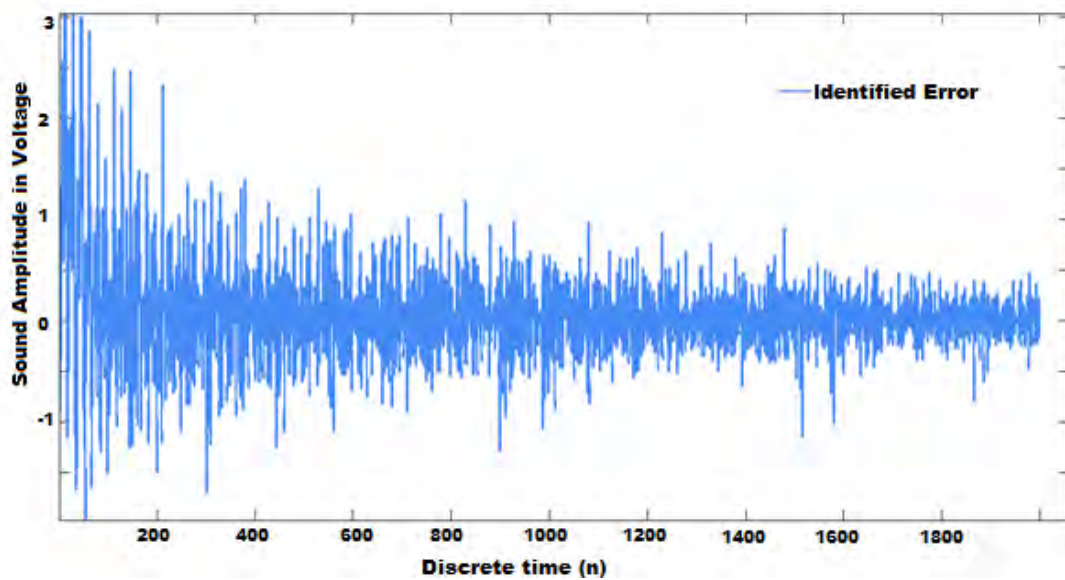

Figure 3.9: Identified Error for an AC motor operating at 820 RPM
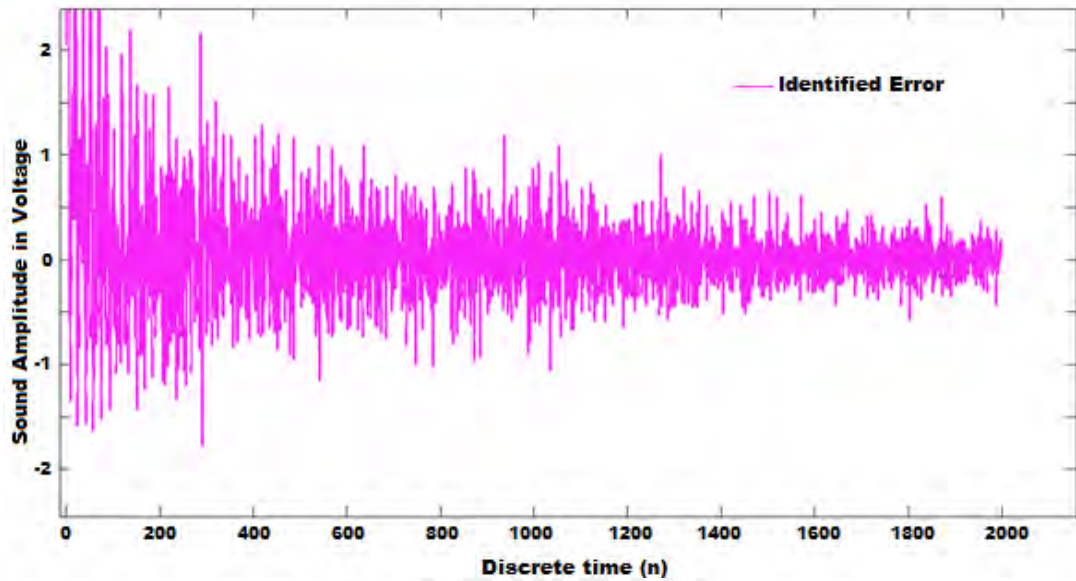
Figure 3.10: Identified Error for an AC motor operating at 1093 RPM

3.2 EXPERIMENTAL ANALYSIS ON DC MOTOR USING REAL-TIME SYSTEM

Hardware configuration is depicted in Figure 3.11: a single speaker and microphone next to the DC motor are used for this analysis. Control is made using an FPGA programmed in LabVIEW and results are shown for different speeds. As it were mentioned, there is an offset caused between noise and error.
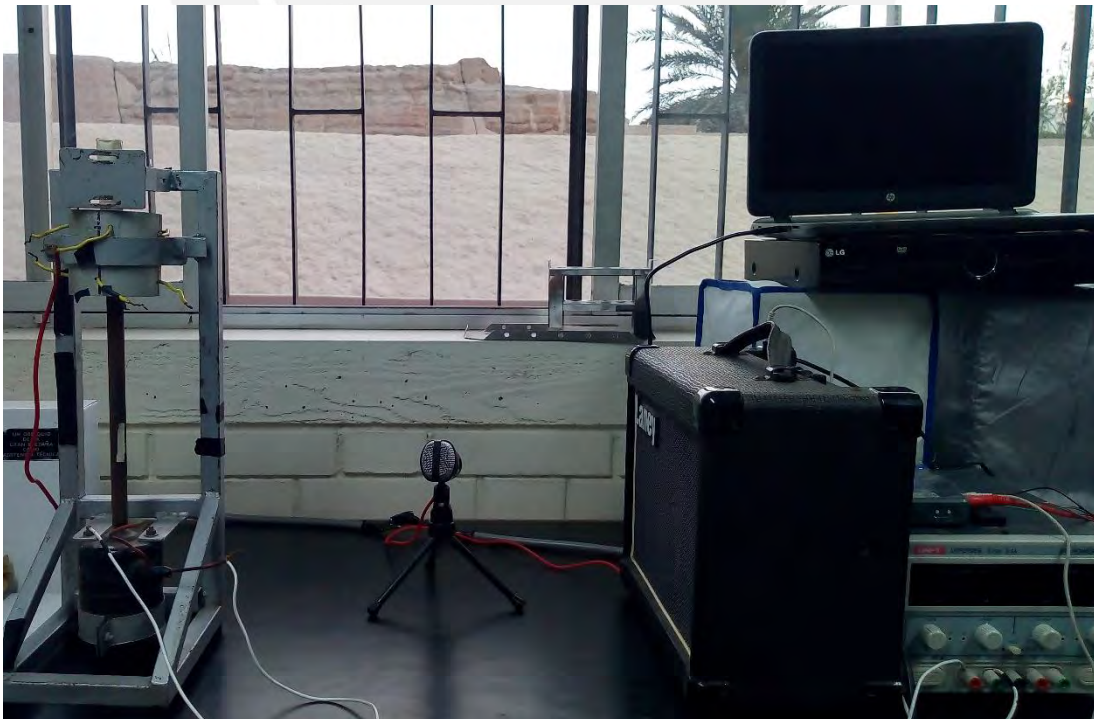
Figure 3.11: Hardware settings for system identification on DC motor

For this analysis, the experiment is made using the motor operating in its two nominal speeds: 1000 RPM (low speed) and 2000 RPM (high speed).

Figure 3.12: Experiment at low speed
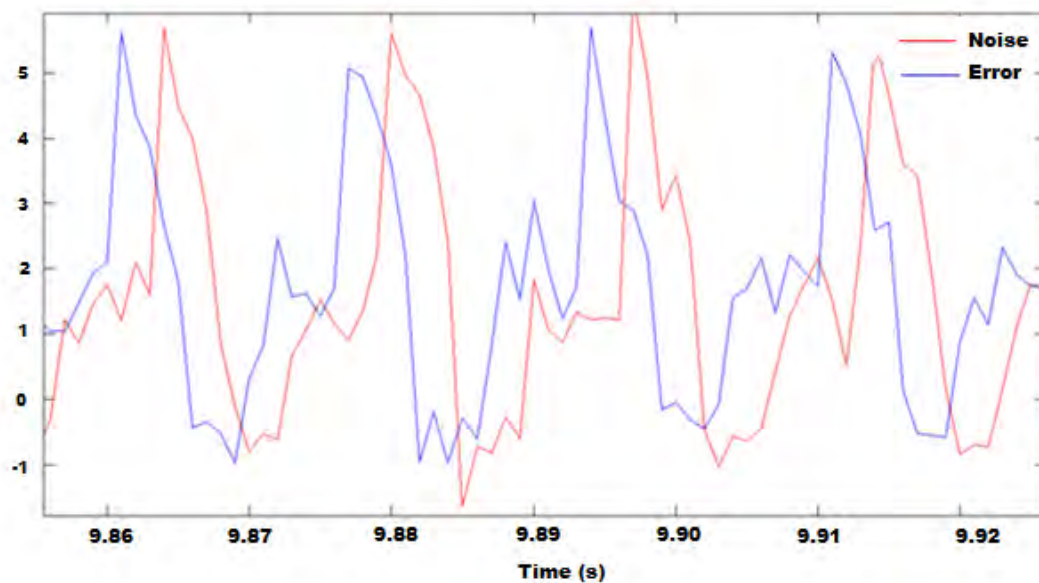
Figure 3.13: Experiment at high speed

It is evident that the speaker should replicate the exact noise produce by motor, but an offset between noise and error is noticed and it could explain why sometimes noise is increasing instead of reducing.

26

3.3 EXPERIMENTAL ANALYSIS ON INTERNAL COMBUSTION ENGINE

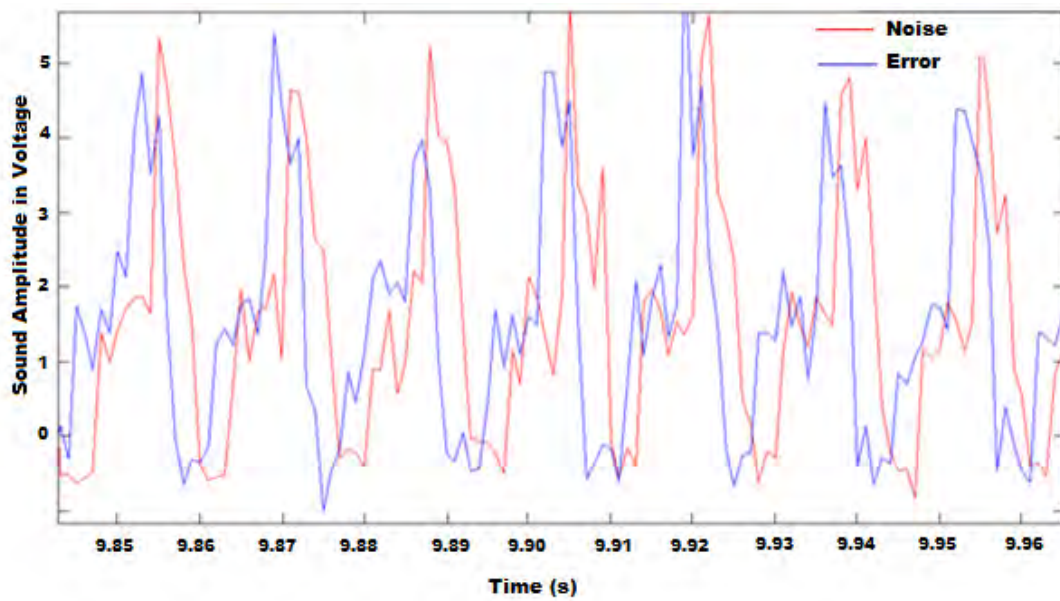For this analysis a Diesel Engine (shown in Figure 3.14) is tested under 2000 RPM. In this case, a PC is used to do the control which means it is not a Real Time System. A single speaker and microphone are used as well. Test, as the rest of experiment in this chapter, consist on sending inverse signal and no control is executed.

Figure 3.14: Diesel engine for analysis (Energy Laboratory, PUCP)

Figure 3.15: Diesel Engine Test at 2000 RPM

Results demonstrate that using an inverse signal to supressed noise is not enough to achieve active noise cancellation. In some cases, noise levels are increased. For this reason, adaptive control is necessary.
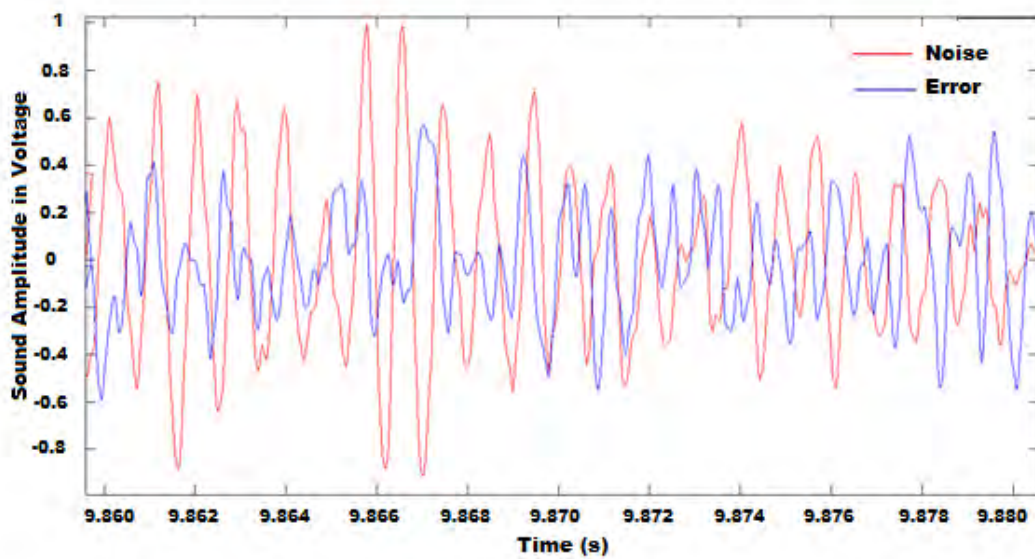
4. EXPERIMENTAL RESULTS

In this chapter the Least-Mean-Square algorithm is tested for different cases to probe its efficacy and monitoring minimal and maximum attenuation.

4.1 PROPOSED ALGORITHM

The proposed algorithm for this work is a hybrid feedback/feedforward FXLMS control algorithm as it is shown in Figure 4.1. This work takes some references from different authors that uses FXLMS as Chen, Chang, & Kuo (2017), for instance. However, the algorithm performs an offline identification of the characteristics of motor/engine using LMS and adaptive coefficient "C".

Although both "A and "C" coefficients, which depend on the feedback and feedforward configuration, control the error through the secondary path effect "S" for every instant "n"; "C" is in charge of performing offline identification that makes easier to achieve noise cancellation.
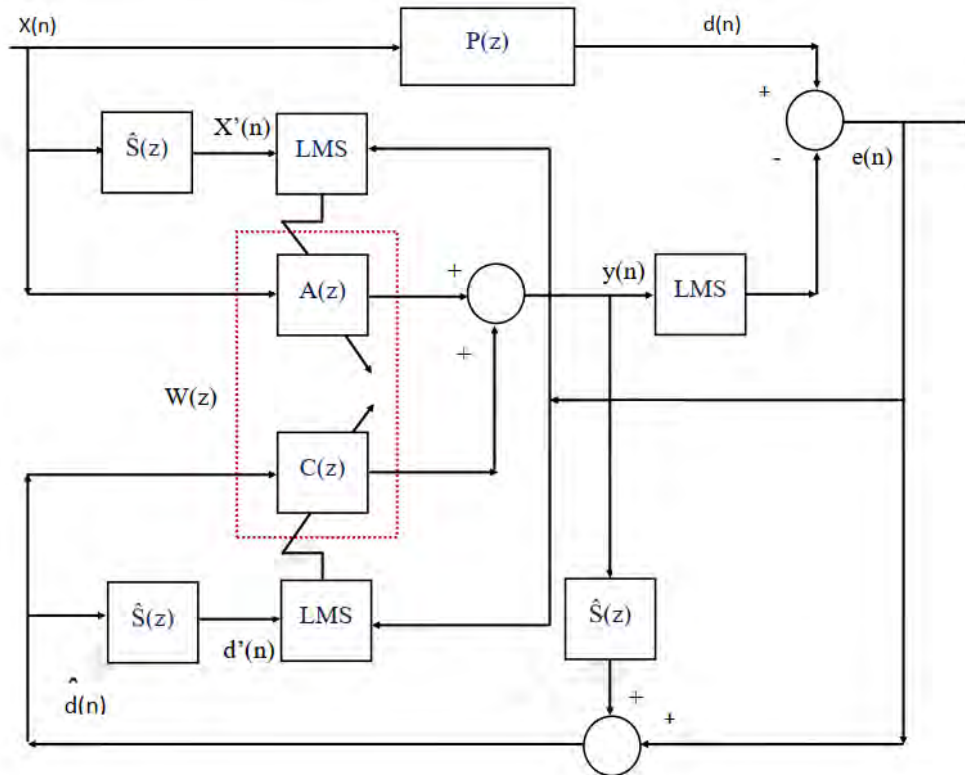
Figure 4.1: Feedforward/feedback diagram scheme (Calderón, Lengua et all., 2019)

4.2   CODE FOR ALGORITHM

As a consequence of the analysed mathematical model in previous chapter, the algorithm was possible to design in pursuance of achieving noise cancellation, which is based on the capacity to execute the LMS loop through a recurrence of main algorithm. Hence, the explanation of this design is described in the following sub chapters.

4.2.1   FLOW DIAGRAM

In the following figure is depicted the algorithm design by flow chart.

Figure 4.2: Flow chart of the algorithm design

4.2.2   PSEUDOCODE FOR THE ALGORITHM

The following text describes the algorithm design by pseudocode, where *w* is the weight matrix, *Sx* is the secondary path, *μ* is the adjusting coefficient, *X* is the input signal, *Sy* is the updated secondary path and *n* is the discrete time domain.

//LMS code

Process Start_Variables

  w → zeros(1,16) // weight matrix

  Sx→ zeros(1,16) // 2 bytes auxiliar array

  μ → 0.1;

  Error → 0;

End Initialize variable

Process Least mean-square loop

  X(n) → ADC(Microphone Signal)

  Sx → [X(n) Sx(n-1)]

  Sy → $\sum_{k=0}^{16} w_k . Sx_k$

  Error → X(n) - Sy

  W(n) → W(n) + μ . error . Sx

End Loop

4.3 EXPERIMENTS ON ELECTRICAL MOTORS AND ENGINES

DC motor joined to an Active magnetic Bearing system, shown in Figure 4.3 , is tested according to previous data taken from system identification. Additionally, it is observed a relation between vibration, which is the source of sound, and noise produced as consequence of it (Calderón, et al., 2019).

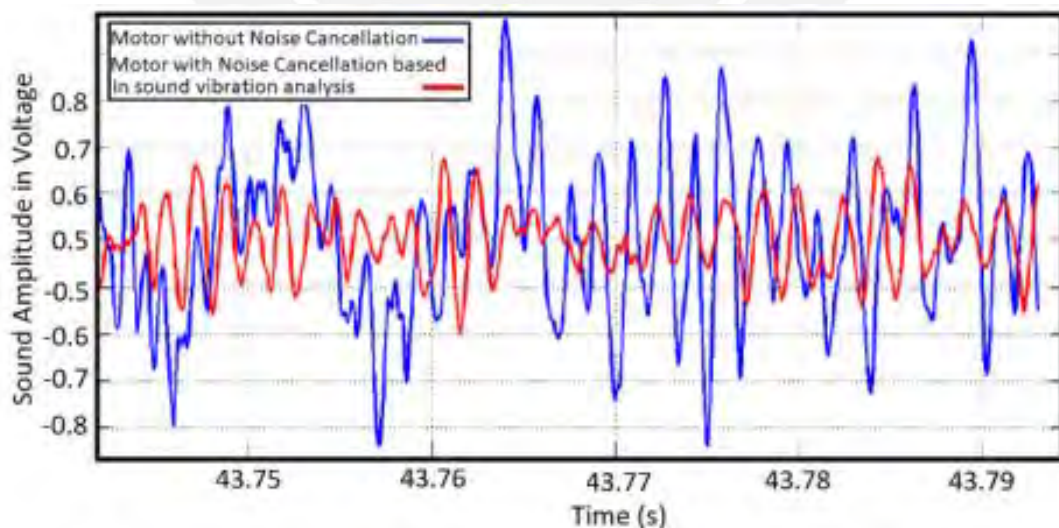
Figure 4.3: Setup for experimental test on a DC motor

Figure 4.4: Experimental test in time domain for DC motor (Calderón, Lengua, Lozano, et all., 2019)

A Diesel Engine depicted in Figure 4.5 is also tested with the proposed algorithm. Engine operates around 1000 - 2000 RPM and produced 80 dB in analysed area. A maximum attenuation of 43 dB is achieved. Figure 4.6 shows an extract of the resultant graph.

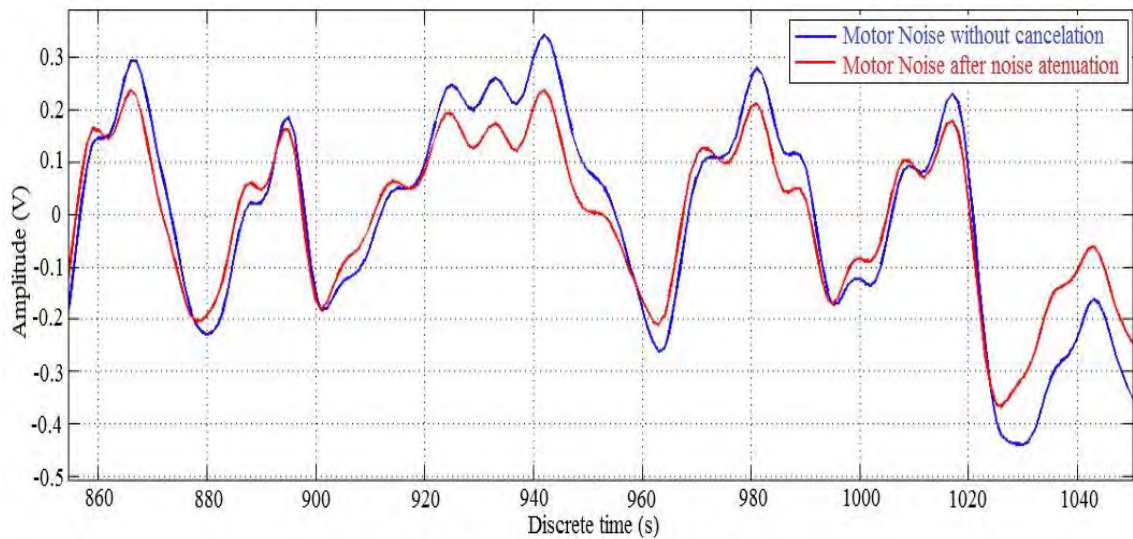Figure 4.5: Diesel Engine tested with the algorithm (Energy Laboratory, PUCP)

Figure 4.6: Noise Signal and noise cancellation based on LMS for an Engine (Calderón, Lengua, et all., 2019)

Additionally, AC motor joined to an active magnetic bearing, shown in Figure 4.7, is tested for different speeds. Speed is controlled via frequency inverter in order to work at 3000 RPM and 200 RPM. Figure 4.8 exhibits results at 3000 RPM, 11 dB attenuation is accomplished. On the other hand, 24 dB attenuation is achieved at 200 RPM (Figure 4.9). In this experiment, room was isolated in a way that harmonics can be reduced.

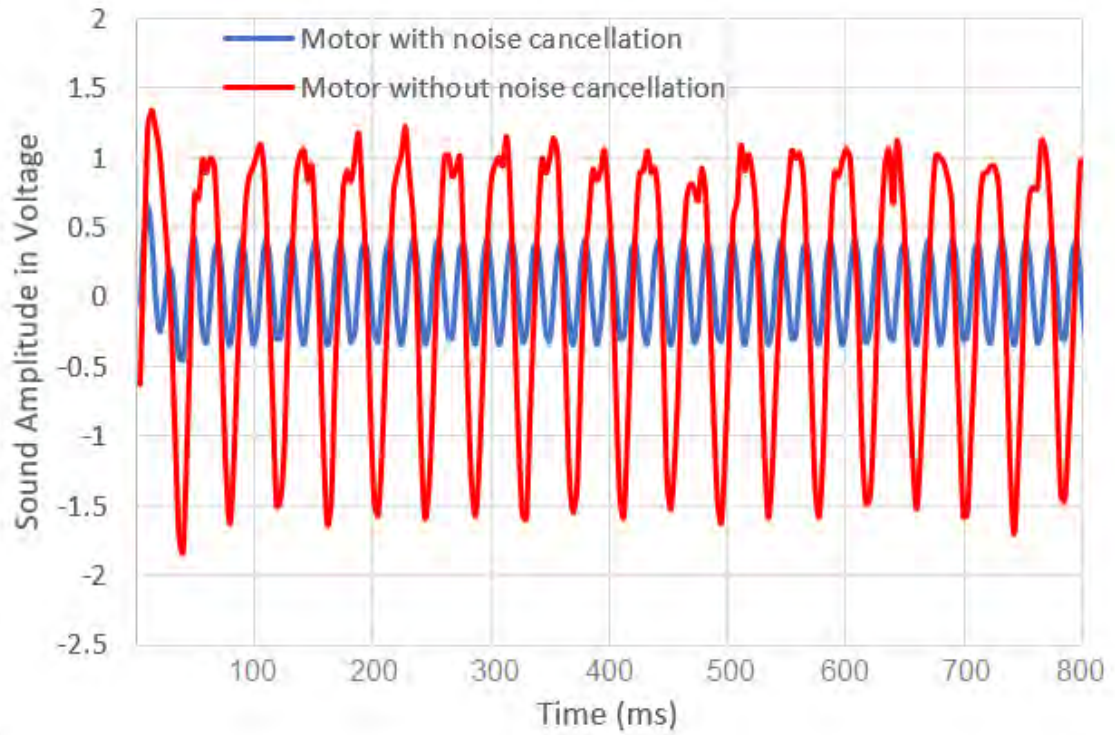Figure 4.7: Setup for experimental test on AC motor

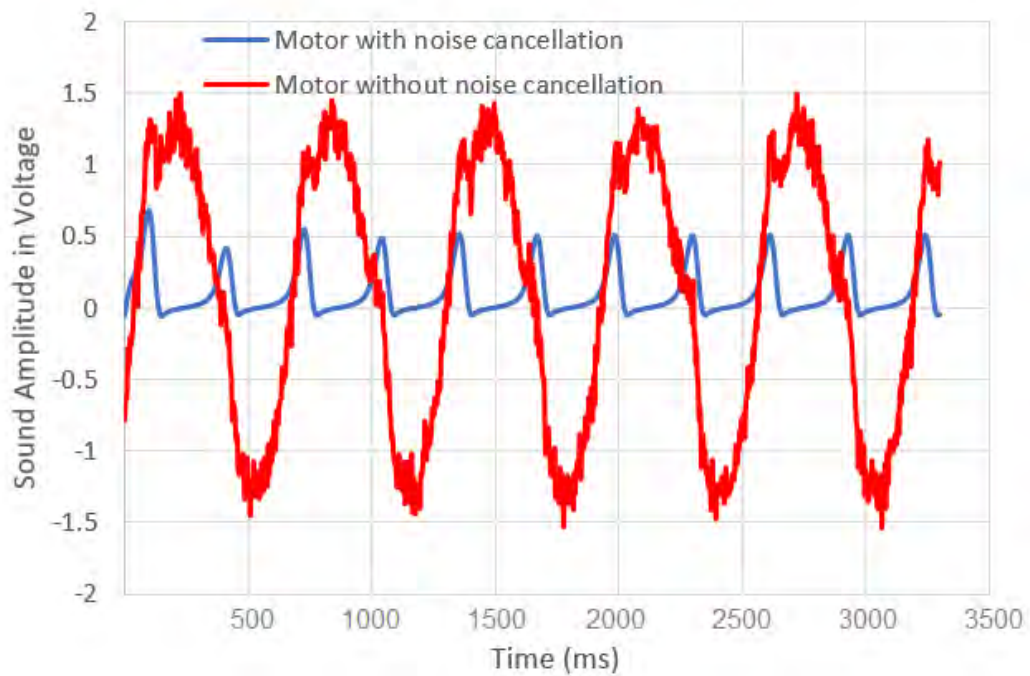Figure 4.8: Obtained results on AC motor at 3000 RPM

Figure 4.9: Obtained results on AC motor at 200 RPM

35

CONCLUSIONS AND RECOMMENDATIONS

An attenuation algorithm for motors and engines in the operation range from 200 to 3000 rpm has been presented supported on experiments and simulations based on Least-Mean-Square.

The proposal has been verified in experimental conditions and a minimum attenuation of 10 dB has been accomplished for motors at 200 to 3000 RPM

The main advantage of adaptive systems is that they are able to tune the parameters of the controller automatically. However, they require a model estimation of the plant. It means a preliminary study is necessary in order to guarantee efficacy.

Results shows that in order to get a better effect, hybrid active and passive noise cancellation should be used simultaneously as they complement each other. Effects of both systems must be analysed in systems that work in variable frequency.

Algorithm with real time controllers would improve results with rotating machines that are continuously changing their parameters as they can be faster enough to work under these circumstances.
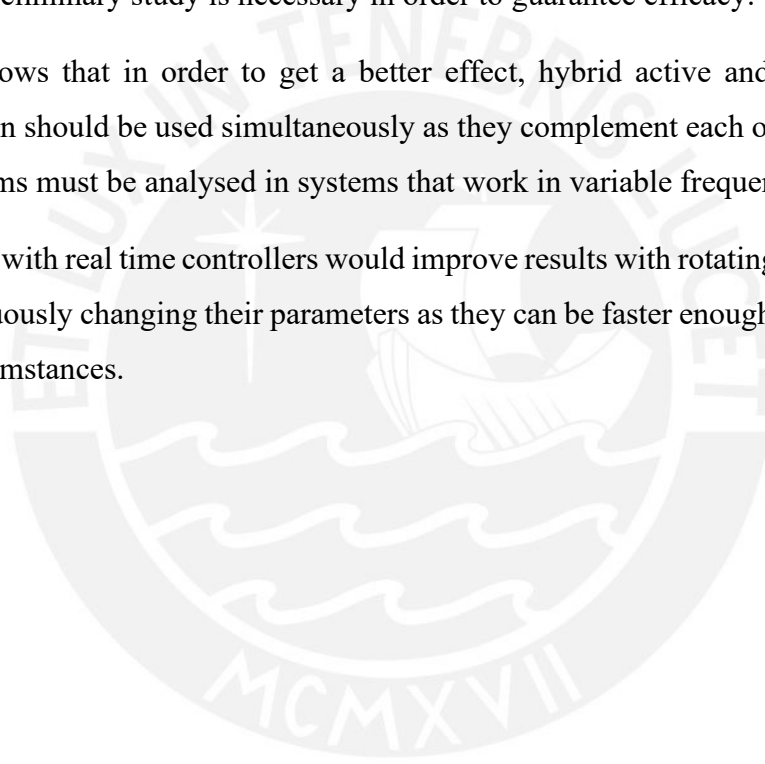
References

Ardekani, I. T., Sharifzadeh , H., Rehman, S. & Abdulla, W. H., 2015. Efficient FXLMS Algorithm with Simplified Secondary Path Models. *IEEE International Conference on Acoustics, Speech and Signal Processing (ICASSP).*

Bies, D. A. & Hansen, C. H., 2003. *Engineering Noise Control: Theory and Practice.* Third edition ed. s.l.:Spoon Press.

Calderón Chavarri, J. A., 2015. *Analysis and implementation of active noise control strategies using piezo and EAP actuators.* Lima: PUCP.

Calderón, J. A., Tafur, J. C., Barriga, E. B. & Lozano, J. H., 2019. Active Noise Control Proposal for Rotating Machines. *International Institute of Informatics and Systemics.*

Calderón, J. A. et al., 2019. Active Noise Control proposal design enhanced because of using sensors/actuators based on nanostructures. *E3S Web Of Conferences 95, 01003.*

Chen, K.-C., Chang, C.-Y. & Kuo, S. M., 2017. Active noise control in a duct to cancel broadband noise. *Materials Science and Engineering.*

Diniz, P. S. R., 2008. *Adaptive Filtering, Algorithm and Practical Implementation.* Boston, MA: Springer.

Elliot, S. J. & Nelson, P. A., 1993. Active Noise Control. *IEEE Signal Processing Magazine,* October.

Farhang-Boroujeny, B., 2013. *Adaptive Filters: Theory and Applications.* s.l.:Wiley.

Hansen, C. H., 2001. *Understanding Active Noise Cancellation.* London: Spon.

Jing, F., 2010. Active Noise Control System of Central Pump House In Mine Tunnel. *International Conference on Measuring Technology and Mechatronics Automation.*

Keelara Veerappa, M. P. & Venugopalachar, S., 2011. The possible influence of noise frequency components on the health of exposed industrial workers - A review. *Noise & Health,* pp. 16-25.

Kuo, S. M. & Morgan, D. R., 1999. Active Noise Control: A Tutorial Review. *Proceedings of the IEEE,* 87(6).

Kuo, S. M. & Morgan, D. R., 2000. Review of DSP Algorithms for Active Noise Control. *International Conference on Control Applications.*

Luo, L., Sun, J., Huang, B. & Bai, Z., 2017. An Adaptive Recursive Feedback Active Noise Control System for Chaotic Noise. *International Conference on Control, Automation and Robotics.*

Mohapatra, S. & Kar, A., 2015. An Advanced Feedback Filtered-x Least Mean Square Algorithm for Wideband Noise Removal. *12th International Conference on Electrical Engineering/Electronics, Computer, Telecommunications and Information Technology (ECTI-CON).*

Möser, M., 2009. *Engineering Acoustics.* Berlin Heidelberg: Springer-Verlag.

Municipalidad de Lima, 2019. [Online] Available at: http://smia.munlima.gob.pe/mapa-tematico/detalle/113 [Accessed 13 Marzo 2021].

Ordaz, E. et al., 2009. Effects of noise exposure in working places on quality of life and performance. *Medicina y Seguridad del Trabajo,* 55(216).

Organismo de evaluación y fiscalización ambiental, 2016. La contaminación sonora en Lima y Callao.

Presidencia del Consejo de Ministros, 2003. DECRETO SUPREMO Nº 085-2003-PCM. 31 Enero.

Sookpuwong, C. & Chompoo-Inwai, C., 2017. Performance Comparisons between A Single-Channel Feedforward ANC System and A Single-Channel Feedback ANC System in A Noisy-Enviroment Classroom. *Conference Proceedings of ISEIM 2017,* pp. 203-206.

Streeter, A. D., Ray, L. R. & Collier, R. D., 2004. Hybrid Feedforward-Feedback Active Noise Control. *American Control Conference.*

Tohyama, M., 2009. *Sound and Signals.* Berlin Heidelberg: Springer-Verlag.

Zangi, K. C., 1994. *Optimal Feedback Control Formulation of the Active Noise Cancellation Problem: Pointwise and Distributed.* Massachusetts: Research Laboratory of Electronics Massachusetts Institute of Technology Cambridge.